J Fluoresc (2014) 24:1067–1076
DOI 10.1007/s10895-014-1386-z

ORIGINAL PAPER

Synthesis, Spectral Characterization, DNA Binding Studies and Antimicrobial Activity of Co(II), Ni(II), Zn(II), Fe(III) and VO(IV) Complexes with 4-Aminoantipyrine Schiff Base of Ortho-Vanillin

B. Anupama · M. Sunita · D. Shiva Leela · B. Ushaiah · C. Gyana Kumari

Received: 4 January 2014 / Accepted: 24 March 2014 / Published online: 30 April 2014

Abstract A series of transition metal complexes of Co(II), Ni(II), Zn(II), Fe(III) and VO(IV) have been synthesized involving the Schiff base, 2,3-dimethyl-1-phenyl-4-(2-hydroxy-3-methoxy benzylideneamino)-pyrazol-5-one(L), obtained by condensation of 4-aminoantipyrine with 3-methoxy salicylaldehyde. Structural features were obtained from their FT-IR, UV–vis, NMR, ESI Mass, elemental analysis, magnetic moments, molar conductivity and thermal analysis studies. The Schiff base acts as a monovalent bidentate ligand, coordinating through the azomethine nitrogen and phenolic oxygen atom. Based on elemental and spectral studies six coordinated geometry is assigned to Co(II), Ni(II), Fe(III) and VO(IV) complexes and four coordinated geometry is assigned to Zn(II) complex. The interaction of metal complexes with Calf thymus DNA were carried out by UV–VIS titrations, fluorescence spectroscopy and viscosity measurements. The binding constants (K_b) of the complexes were determined as 5×10^5 M^{-1} for Co(II) complex, 1.33×10^4 M^{-1} for Ni(II) complex, 3.33×10^5 M^{-1} for Zn(II) complex, 1.25×10^5 M^{-1} for Fe(III) complex and 8×10^5 M^{-1} for VO(IV) complex. Quenching studies of the complexes indicate that these complexes strongly bind to DNA. Viscosity measurements indicate the binding mode of complexes with CT DNA by intercalation through groove. The ligand and it's metal complexes were screened for their antimicrobial activity against bacteria. The results showed the metal complexes to be biologically active, while the ligand to be inactive.

Keywords Metal complexes · Schiff bases · 4-aminoantipyrine · Antimicrobial activity · DNA binding

B. Anupama (✉)
Department of Chemistry, R.B.V.R.R. Women's College, Narayanaguda, Hyderabad, India
e-mail: anupama_gudi@yahoo.co.in

M. Sunita
Department of Chemistry, Govt. Polytechnic for Women, Medak, Andhra Pradesh, India

D. Shiva Leela · B. Ushaiah · C. Gyana Kumari
Department of Chemistry, Osmania University, Hyderabad 500007, India

Introduction

The Schiff bases of 4-aminoantipyrine and its complexes have variety of applications in the biological, clinical, analytical and pharmacological fields [1–6]. It is known that some drugs showed increased activity when administered as metal chelates rather than as organic compounds. The coordinating property of 1-phenyl-2,3-dimethyl-4-aminopyrone (4-amino antipyrine) can be modified into a flexible ligand system by condensation with a variety of reagents like aldehydes, ketones, thiosemicarbazides, carbazides etc. [7–15]. A number of metal chelates are of current interest due to their important applications in nucleic acid chemistry as DNA probes of DNA structure in solutions, reagents for the mediation of strand scission of duplex nucleic acid under physicochemical conditions and as chemotherapeutic agents and in the genomic research.

The interaction between DNA and transition metal complexes is an important fundamental issue in life sciences. These complexes can bind to DNA in non-covalent modes such as electrostatic, intercalative and groove binding. The above applications require that the complex binds to DNA through an intercalate mode, where in, the planar aromatic heterocyclic group is inserted and stacked between the base pairs of DNA. The mode is related to in-vivo replication and transcription of DNA, mutation of genes, variations of species in their character and to the action mechanism of some

synthetic chemical nucleases. Considering the relevance and significance of Schiff base complexes in DNA binding, we report the synthesis, characterization, DNA binding and antibacterial activity studies of Co(II), Ni(II), Zn(II), Fe(III) and VO(IV) complexes of Schiff base (2,3-dimethyl-1-phenyl-4-(2-hydroxy-3-methoxybenzylideneamino)-pyrazol-5-one) derived from 4-aminoantipyrine and ortho-vanillin.

Experimental

All the chemicals used were of AR grade. 4-Aminoantipyrine, metal salts, 3-methoxy salicylaldehyde, Tris–HCl, Ethidium bromide (EB) and CT DNA. They were purchased from Sigma Aldrich chemicals. All other chemicals and solvents were of analytical reagent grade and used without further purification. Millipore water was used for preparing buffer.

All the experiments involving with the interaction of the ligand and complexes with CT DNA were carried out in tris buffer (5 mM Tris–HCl, 50 mM NaCl, pH 7.0). The solution of CT-DNA in the buffer gave ratios of UV absorbance of about 1.8–1.9:1 at 260 nm and 280 nm indicating its purity. DNA concentration per nucleotide was determined by absorbance at 260 nm by using molar extinction coefficient (6,600 M^{-1} cm^{-1}) [16]. The ligands and complexes were dissolved in a solvent mixture of DMSO and Tris–HCl buffer at the concentration 1.0×10^{-5} M. The stock solution of DNA was stored at 4 ° C and used within 5 days, because continues freezing of DNA causes precipitation.

Physical Measurements

Elemental analysis of the ligand and it's metal complexes was carried out using a Perkin-Elmer 240C (USA) elemental analyser. Molar conductances of the metal complexes were measured in DMSO solution, using Digisun digital conductivity meter. Magnetic susceptibilities of the complexes were measured on Guoy balance, model 7550, using Hg $[Co(NCS)_4]$ as standard. The diamagnetic corrections of the complexes were done using Pascal's constants. Thermo gravimetric analysis of the complexes were carried on Shimadzu DTG-60H system in the temperature range of 0–1,000 °C. Melting points of the ligand and m.p/decomposition temperature of complexes were determined on Polmon instrument (MP-96). IR spectra were recorded in KBr discs on Brucker FT-IR spectrometer from 400 to 4,000 cm^{-1}. Electronic spectra were recorded with Elico SL 159 UV-Visible Spectrophotometer from 200 to 1,100 nm. ^1H NMR spectra were recorded in $CDCl_3$, on Brucker 400 MHz spectrometer. The mass spectra were recorded by ESI technique on LCQ ion trap thermo Finningan Sanjose CA (USA) mass spectrometer.

Synthesis of Ligand

Ligand(L) [2,3-Dimethyl-1-Phenyl-4-(2-Hydroxy-3-Methoxy Benzylideneamino)-Pyrazol-5-One]

A mixture of 4-aminoantipyrine (0.05 mol) and 3-methoxy salicylaldehyde (0.05 mol) in ethanol, on refluxing for 2 h, with constant stirring, resulted in dark yellow solid product. It was filtered, washed with petroleum ether and recrystallized in ethanol. Purity of the resultant Schiff base compound was checked by TLC. Yield: 85–90 % [17] (Scheme 1).

Synthesis of Complexes

In the preparation of the metal complexes, the metal and the ligands were mixed in 1:2 molar ratio using required quantities of ethanol. Hot ethanolic solution of ligand (0.01 mol) and hot ethanolic solution of corresponding metal salts (0.005 mol) (MX_2, where M=Co(II), Ni(II), Zn(II), Fe(III) and VO(IV); X=chlorides/nitrates; for VO(IV);X=SO_4) were mixed together, refluxed for 2–3 h and left for evaporation at room temperature for 3 days. Coloured solid metal complexes were obtained. The products were filtered, washed with cold ethanol and dried under vacuum over calcium chloride.

$[Co(3\text{-}OMe\ SALAAP)_2]H_2O$

IR $_{max}$: 3,387 cm^{-1}($\nu_{O\text{-}H/H2O}$), 1,636 cm^{-1} ($\nu_{C=N}$), 1,664 cm^{-1} ($\nu_{C=O}$), 1,385 cm^{-1} ($\nu_{C\text{-}O}$), 547 cm^{-1} ν_{M-O}, 466 cm^{-1} (ν_{M-N}) Anal.Calc for $C_{38}H_{36}N_6CoO_6$ Cal: C 62.21, H 4.91, N 11.45 :found :C 62.25, H 4.93, N 11.46;μ_{eff} : 4.92BM UV–vis(nm) 307,397, 497, 670 :ESI-MS (m/z): 732, $[Co(L)_2]^+$

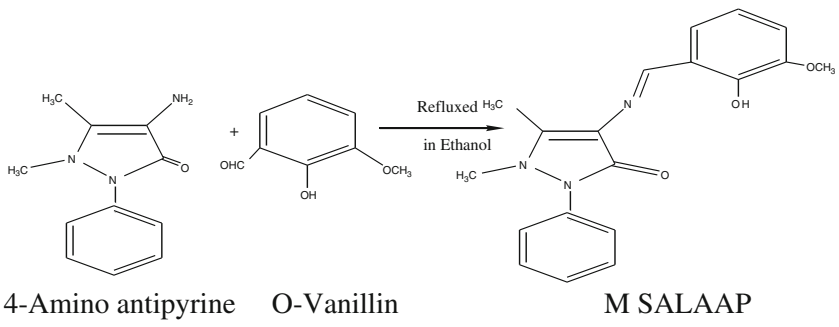

Scheme 1 Reaction scheme for the synthesis of ligand (L)

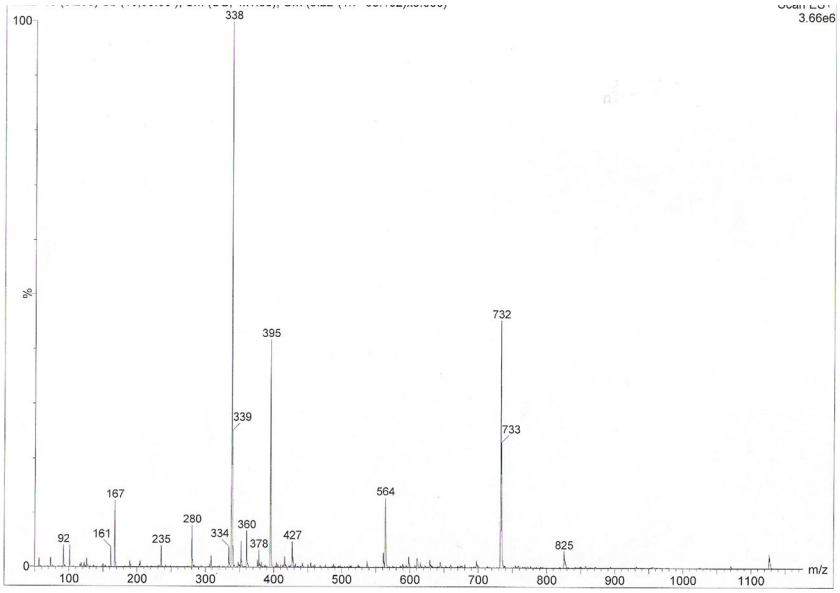

Fig. 1 Mass spectrum of Co(II)-M SALAAP

[Ni(3-OMe SALAAP)$_2$]H$_2$O

IR $_{max}$: 3,377 cm^{-1}($\nu_{O-H/H2O}$), 1,604 cm^{-1} ($\nu_{C=N}$), 1,664 cm^{-1} ($\nu_{C=O}$), 1,381 cm^{-1} (ν_{C-O}), 547 cm^{-1} ν_{M-O}, 466 cm^{-1} (ν_{M-N}) Anal.Calc for C_{38} H_{36} N_6 Ni O_6 Cal: C 62.12, H 5.12, N 11.51 :found :C 62.46, H 4.90, N 11.44;μ_{eff} : 2.79 BM UV–vis(nm) 312,345, 467, 762 :ESI-MS (m/z): 731 $[Ni(L)_2]^+$

[Zn(3-OMe SALAAP)$_2$]H$_2$O

IR $_{max}$: 3,398 cm^{-1}($\nu_{O-H/H2O}$), 1,600 cm^{-1} ($\nu_{C=N}$), 1,665 cm^{-1} ($\nu_{C=O}$), 1,372 cm^{-1} (ν_{C-O}), 546 cm^{-1} ν_{M-O}, 465 cm^{-1} (ν_{M-N}) Anal.Calc for $C_{38}H_{36}N_6ZnO_6$ Cal: C 61.70, H 4.87, N 11.36 :found :C 61.73, H 4.86, N 11.38; :ESI-MS (m/z): 737, $[Zn(L)_2]^+$

[Fe(3-OMe SALAAP)$_2$]H$_2$O

IR $_{max}$: 3,387 cm^{-1}($\nu_{O-H/H2O}$), 1,636 cm^{-1} ($\nu_{C=N}$), 1,664 cm^{-1} ($\nu_{C=O}$), 1,385 cm^{-1} (ν_{C-O}), 547 cm^{-1} ν_{M-O}, 466 cm^{-1} (ν_{M-N}) Anal.Calc for $C_{38}H_{36}N_6CoO_6$ Cal: C 62.21, H 4.91, N 11.45 :found :C 62.25, H 4.93, N 11.46; :ESI-MS (m/z): 732, $[Co(L)_2]^+$

[VO(3-OMe SALAAP)$_2$]H$_2$O

IR $_{max}$: 3,413 cm^{-1}($\nu_{O-H/H2O}$), 1,582 cm^{-1} ($\nu_{C=N}$), 1,663 cm^{-1} ($\nu_{C=O}$), 1,382 cm^{-1} (ν_{C-O}), 547 cm^{-1} (ν_{M-O}),

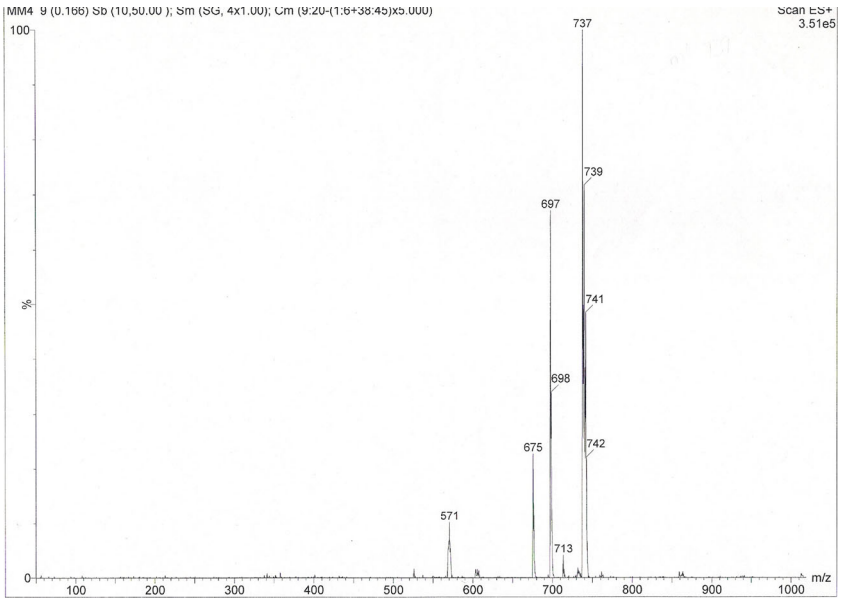

Fig. 2 Mass spectrum of Zn(II)-M SALAAP

Table 1 Mass spectral data of ligand and its complexes

Compound	Calculated mass	Obtained mass m/z	Peak assigned
Ligand(L)	337	338	M+1
Ni(II) complex	730	731	M
Co(II) complex	730	732	M+1
Zn(II) complex	737	737	M,M+2
Fe(III) complex	764	765 M+1	
VO(IV) complex	756	737	M-H_2O

465 cm^{-1} (ν_{M-N}) 964 cm^{-1} ($\nu_{V=O}$), Anal.Calc for $VOC_{38}H_{38}N_6O_7$ Cal: C 60.31, H 5.06, N 11.11 :found :C 60.34, H 5.12, N 11.19; :ESI-MS (m/z): 737, $[VO(L)_2]^+$-H_2O

DNA Binding Studies

Absorption Spectra

Absorption spectra were recorded on Elico SL 159 UV-Visible spectrophotometer using 1 cm quartz microcuvettes. Absorption titrations were performed by keeping the concentration of the complex constant (10 μM) and by varying the concentration of CT–DNA from 10 to 100 μM. For the complexes, the binding constants (K_b), have been determined from the spectroscopic titration data using the following Eq. 1.

$$[DNA]/(\varepsilon_a-\varepsilon_f) = [DNA]/(\varepsilon_b-\varepsilon_f) + 1/K_b(\varepsilon_b-\varepsilon_f) \quad (1)$$

The apparent extinction coefficient ε_a, was obtained by calculating A_{obs}/[complex], ε_f and ε_b correspond to the extinction coefficient for the free (unbound) and fully bound complex respectively. A plot of [DNA]/($\varepsilon_a-\varepsilon_f$) vs. [DNA] will have a slope equal to 1/($\varepsilon_b-\varepsilon_f$) and an intercept equal to 1/K_b($\varepsilon_b-\varepsilon_f$), K_b is then given by the ratio of the slope and the intercept.

Fluorescence Titration

To understand the interaction pattern of the complexes with DNA, fluorescence titration method was used. Fluorescence measurements were carried out by keeping the concentration of complexes constant (15 μM), and concentrations of CT DNA varied from 10 μM to 100 μM. An excitation wavelength of 335 nm was used.

Viscosity Measurements

Viscometric titrations were performed with an Ostwald viscometer maintained at room temperature. The flow times were measured with a digital timer and each sample was measured five times for accuracy and an average flow time was calculated. Data was presented as $(\eta/\eta_o)^{1/3}$ versus [complex]/[DNA], where η is the viscosity of DNA in the presence of complex and η_o is the viscosity of DNA alone. Viscosity values were calculated from the observed flow time of DNA containing solutions(t) corrected that buffer alone (t_o). $\eta=t-t_o$.

Antibacterial Study

The antibacterial activity of the complexes was studied against Gram-positive bacteria *Staphylococcus aureus* and Gram-negative bacteria *Escherichia coli*. The solutions of metal complexes and ligand were prepared in DMSO at a concentration of 200 μg/ml, 100 μg/ml, and 50 μg/ml. Paper discs of whattman filter paper no.1 were sterilized in an autoclave and saturated with solution of metal complexes in DMSO or DMSO as a negative control and were placed aseptically in the petridishes containing nutrient agar media inoculated with the above mentioned two bacteria separately. The petridishes were incubated at 37 °C and the inhibition zones were recorded after 24 h of incubation period.

Results and Discussion

The Schiff base ligand, 2,3-dimethyl-1phenyl-4-(2-hydroxy-3-methoxybenzylideneamino)-pyrazol-5-one (M SALAAP) was yellow coloured solid and is stable at room temperature. It is soluble in ethanol and dimethyl sulphoxide (DMSO).

The complexes of Co(II), Ni(II), Zn(II), Fe(III) and VO(IV) with M SALAAP ligand were found to be stable at room temperature and non hygroscopic. They are insoluble in water, but soluble in DMSO and ethanol. All the complexes were characterized by various spectral and analytical methods.

Table 2 IR Absorption frequencies of free ligand and their metal complexes (in cm^{-1})

Ligand/complex	OH/H2O	C=N	C=O	C–O	M–O	M–N	V=O
Ligand	2,826	1,598	1,663	1,364	–	–	–
Ni(II) complex	3,377	1,604	1,664	1,381	547	466	–
Co(II) complex	3,387	1,636	1,664	1,395	547	466	–
Zn(II) complex	3,398	1,608	1,664	1,372	546	465	–
Fe(III) complex	3,386	1,585	1,663	1,365	547	466	–
VO(IV) complex	3,413	1,582	1,664	1,382	547	465	964

Table 3 Electronic absorption spectral and magnetic moment data of complexes

Compound	Maximum absorption wavelength (in nm)	Band assignment	Magnetic moment μ (B.M)	Geometry
Ligand	302,342,402	INCT	–	–
Ni(II) complex	312,345	INCT		
	467	$^3A_{2g}(F)\rightarrow{}^3T_{1g}(p)$	2.79	Octahedral
	762	$^3A_{2g}(F)\rightarrow{}^3T_{1g}(F)$		
Co(II) complex	307,397	INCT		
	497	$^4T_{1g}(F)\rightarrow{}^4T_{1g}(p)$	4.92	Octahedral
	670	$^4T_{1g}(F)\rightarrow{}^4T_{2g}(F)$		
Zn(II) complex	–	–	–	Tetrahedral
Fe(III) complex	306,364	INCT	5.65	Octahedral
	464	$^6A_{1g}\rightarrow{}^4T_{2g}$		
	762	$^6A_{1g}\rightarrow{}^4T_{1g}$		
VO(IV) complex	307,339	INCT	1.93	Octahedral
	447	$^2B_2\rightarrow{}^2B_1$		
	567	$^2B_2\rightarrow{}^2A_1$		

Based on the data of elemental analysis and ESI Mass, the composition was assigned to the complexes. The conductance values of all complexes were measured in DMSO solvent. The results suggest, the non-electrolytic nature of complexes in the solvent [18] and also that no anions are present outside the coordination sphere.

^{1}H NMR Spectra and ^{13}C NMR Spectra

The ^{1}H NMR spectrum of ligand (L) displays multiplet signals at 6.8–7.8 δ which are attributed to the aromatic protons. The signal due to the methoxy protons was observed as a singlet at 3.9δ, =C–CH_3 at 2.4 δ, –N–CH_3 at 3.3 δ, and azomethine proton (−CH=N-) at 9.8 δ, intramolecular hydrogen bonded OH group at 13.9 δ as singlets.

The ^{13}C NMR Spectra of the Schiff base ligand is recorded in $CDCl_3$. The azomethine carbon (C_7) gives a peak at 163.7–164.7 δ, =C–CH_3 (C_{10}) at 10.14–10.25 δ, –N–CH_3 (C_{11}) at 35.21–35.61δ, C=O (C_{12}) at 161.7–160.6 δ,−OCH_3(C_{19}) gives a peak at 56.06 δ.

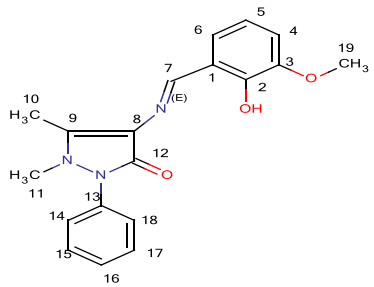

M SALAAP (L)

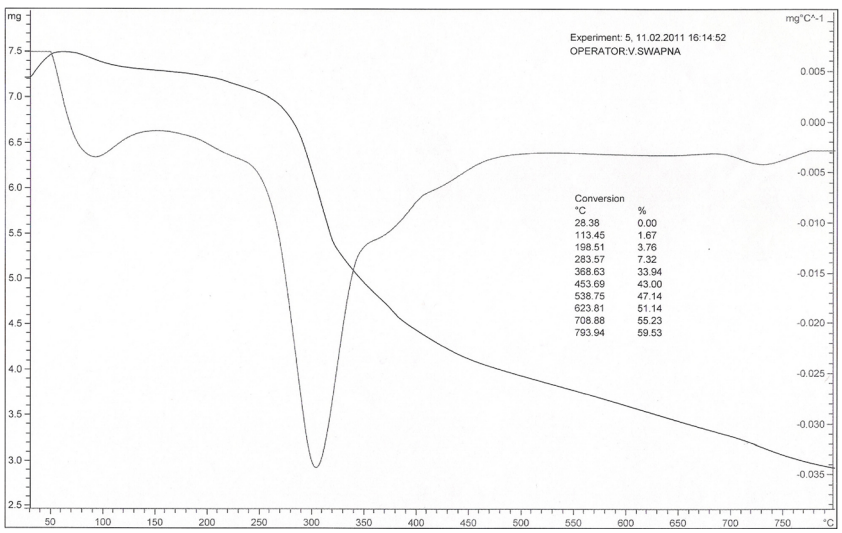

Fig. 3 TGA OF Zn(II)-M SALAAP

Table 4 Antimicrobial activity of complexes (Zone of inhibition in mm)

Compound	*E.coli* 200 μg/ml	Staph 200 μg/ml	*E.coli* 100 μg/ml	Staph 100 μg/ml	*E.coli* 50 μg/ml	Staph 50 μg/ml
`MSALAAP	–	–	–	–	–	–
Ni(II) complex	–	++	–	+	–	–
Co(II) complex	++	++	–	–	–	–
Zn(II) complex	–	+	–	–	–	–
Fe(III) complex	+	+	–	–	–	–
VO(IV) complex	–	+	–	–	–	–
DMSO control	–	–	–	–	–	–

High active = +++ (inhibition zone > 15 mm); Moderately active = ++ (inhibition zone > 10 mm)

Slightly active = + (inhibition zone >5 mm); Inactive = – (Inhibition zone <5 mm)

ESI-MS Spectra and IR Spectra and Type of Bonding

Mass Spectra of complexes provides a vital clue for elucidating the structure of compounds (Figs 1 and 2). The ESI mass of the ligands and its metal complexes recorded at room temperature were used to compare their stoichiometry (Table 1).

The important IR spectral data of the ligand and its complexes are summarized in Table 2. The $_{C=N}$ (of azomethine) observed at 1,598 cm^{-1} in the spectra of the ligand shows a shift by 6–38 cm^{-1} in all the complexes. These are suggestive of the participation of the azomethine nitrogen in coordination [19]. No shift is observed in pyrazol-carbonyl ($_{C=O}$, 1,663 cm^{-1}) band, indicating the non participation of C=O group in coordination with the metal ion. The IR broad bands of metal complexes in the range of 3,377–3,413 cm^{-1} indicate the presence of coordinated/lattice water molecules as also supported by thermal analysis [20–23]. The $_{C-O}$ (phenolic) modes of the ligand appear at 1,364 cm^{-1}, shifted to higher frequency in the complexes indicate the complex formation via deprotonation of phenolic OH [24]. The non ligand bands 546 to 547 cm^{-1} and 465 to 466 cm^{-1} are assigned to $_{M-O}$ and $_{M-N}$ respectively [25]. In addition, the vanadyl complex displays a band at 964 cm^{-1} assignable to V=O modes [26].

Electronic Absorption Spectra and Magnetic Moments

The electronic absorption (UV–VIS) spectra of metal complexes were recorded in DMSO, in the range of 200–1,100 nm and the data is listed in Table 3. The magnetic moment data and the proposed geometry of the complexes are also presented in the same table. These values are closer to the reported complexes [27].

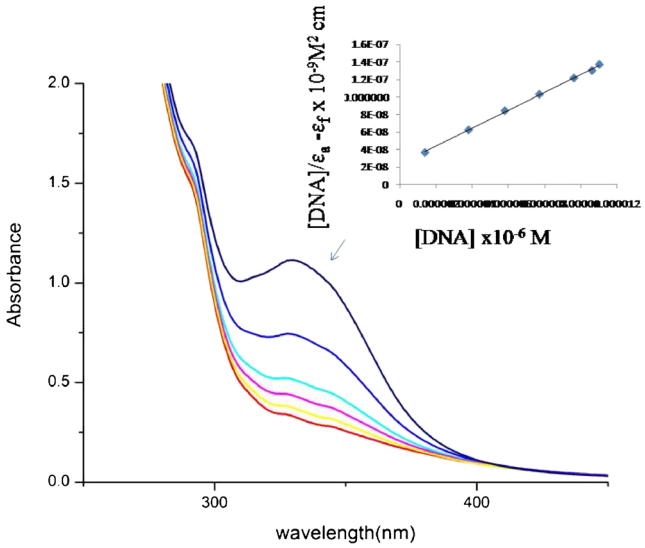

Fig. 4 Absorption spectrum of complex [Co(II)M-SALAAP)] in Tris HCl buffer at 25 °C in the presence of increasing amounts of DNA. Conditions: [Co] =10 μM, [DNA] =10–100 μM. The arrow indicates the change in absorbance upon increasing the DNA concentration. Insert: Plot of [DNA]/($\varepsilon_a - \varepsilon_f$) vs. [DNA]

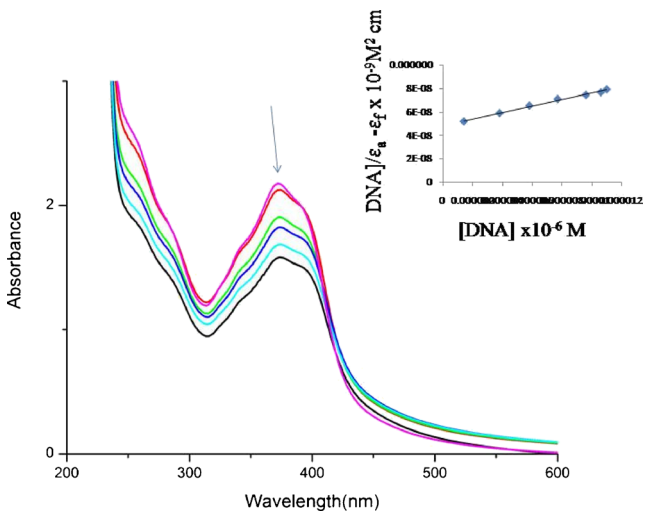

Fig. 5 Absorption spectrum of complex [Ni(II)M-SALAAP)] in Tris HCl buffer at 25 °C in the presence of increasing amounts of DNA. Conditions: [Ni] =10 μM, [DNA] =10-100 μM. The arrow indicates the change in absorbance upon increasing the DNA concentration. Insert: Plot of [DNA]/($\varepsilon_a - \varepsilon_f$) vs. [DNA]

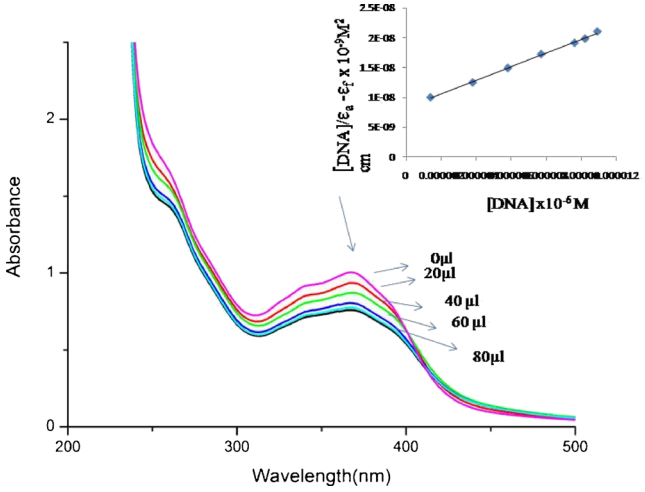

Fig. 6 Absorption spectrum of complex [Fe(III)M-SALAAP)] in Tris HCl buffer at 25 °C in the presence of increasing amounts of DNA. Conditions: [Fe] =10 μM, [DNA] =10–100 μM. The arrow indicates the change in absorbance upon increasing the DNA concentration. Insert: Plot of $[DNA]/(\varepsilon_a-\varepsilon_f)$ vs. [DNA]

Thermal Analysis

Generally, two types of water molecules are associated with the complexes viz, lattice water and coordinated water. The lattice water is lost at low temperature (60–120 °C), where as the coordinated water molecule is lost at high temperatures(150–200 °C) [28].

Thermogram (Fig. 3) of Zn(II)-M SALAAP indicate a total weight loss of 59 % up to 1,000 °C. A small weight loss in the range of 80–100 °C is assigned to loss of lattice water. Maximum and gradual weight loss in the range of 360–1,000 °C is attributable to the decomposition of ligand moiety. The residue at 1,000 ° C indicate the nonvolatile metal component present in the complex. The DTA of the complex showed endothermic peaks at 80°, 310 and 710 °C, which are due to loss of water and subsequent decomposition of the metal complex.

Thermogram of VO(IV)-M SALAAP complex indicate a total weight loss of 56 %, up to 1,000 °C, which occurred in two steps. The maximum and gradual weight loss in the range of 280–330 °C and 390–1,000 °C, are attributable to loss of coordinated water molecule and complete decomposition of the ligand moiety.

Antibacterial Activity

The antibacterial activity of the ligand and it's complexes with Co(II), Ni(II), Zn(II), Fe(III) and VO(IV) have been studied against *E.coli* and *Staphylococcus aureus* by paper disc method. The concentration of these samples were maintained as 200 μg/ml, 100 μg/ml and 50 μg/ml in DMSO. In the present study, the zones of inhibition of antibacterial activity have been presented in Table 4. The results indicate that the Co(II) complexes show highest activity against *E.coli* and *S.aureus* at 100 μg/ml and 50 μg/ml respectively. The mode of action of the compounds may involve in formation of a hydrogen bond through the azomethine group with the active centres of cell constituents, resulting in an interference with the normal functioning of the cell [29]. However, the ligand was found to be biologically inactive. The complexes show antibacterial activity against selected bacteria, results of this work can show that the approach of coordinating 4-aminoantipyrine derivatives with pharmacologically interesting metals could be a suitable strategy to develop novel therapeutic tools for the medicinal treatment.

DNA Binding Studies

In general, complexes with aromatic moieties, which bind to DNA, through intercalation usually results in, hypochromism and bathochromism. This is due to the stacking interaction between aromatic chromophore of the complexes and the base pairs of DNA. The absorption spectra of the complexes, Co(II)-M SALAAP(1), Ni(II)-M SALAAP(2), Zn(II)-M

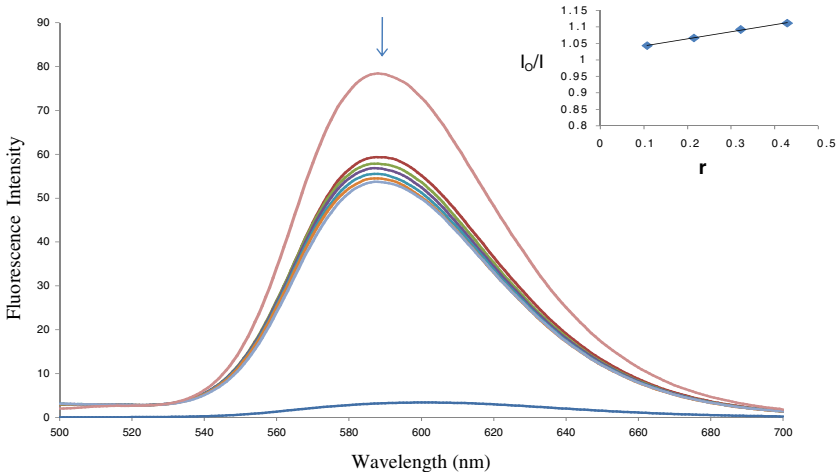

Fig. 7 Emission spectra of EB bound to DNA ([DNA]=2.33× 10^{-5}M). in the absence and presence of Zn(II) complex (10 μM) Inset: Stern-Volmer quenching

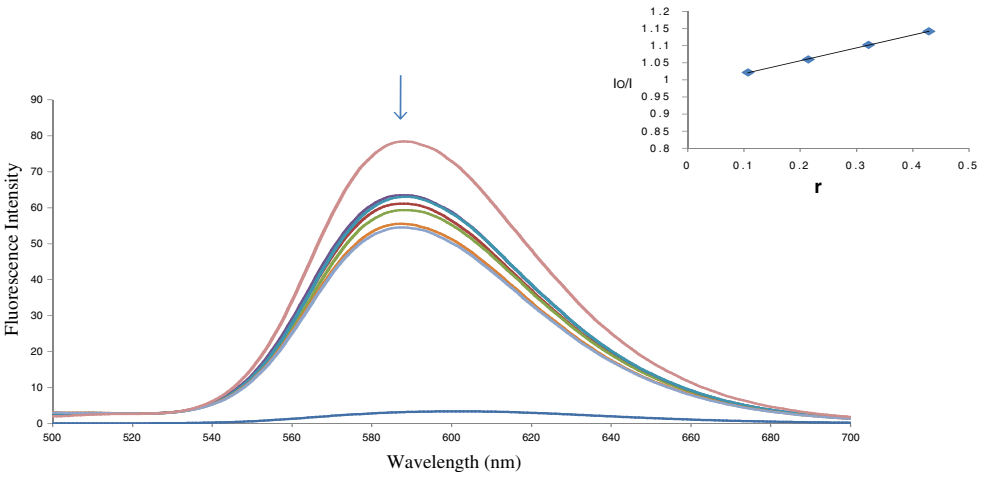

Fig. 8 Emission spectra of EB bound to DNA ([DNA]=2.33×10−5M). in the absence and presence of Co(II) complex (10 μM) Inset: Stern-Volmer quenching

SALAAP (**3**), Fe(III)-M SALAAP(4) and VO(IV)-MSALAAP(5) in the absence and presence of calf thymus DNA are illustrated in Figs. 4, 5, and 6. In the presence of DNA, decrease of peak intensities were observed, in the absorption spectra of complexes.

Hypochromism was suggested to be due to the interaction between the electronic state of the intercalating chromophore and that of the DNA bases. In addition to the decrease in intensity, a small red shift (bathochromism) was also observed in the spectra. These spectral changes are consistent with the intercalation of complexes into the DNA base stack. The plot of the absorption titration data according to Eq. 1 gave a linear plot and resulted in an intrinsic binding constant (K_b) of 5×10^5 M^{-1} for complex **1**, 1.33×10^4 M^{-1} for complex **2**, 3.33×10^5 M^{-1} for complex **3,** 1.25×10^5 M^{-1} for complex **4,** 8×10^5 M^{-1} for complex **5.**

Four metal complexes exhibit a maxima at 601 nm(1), 602 nm(2), 601 nm(3),600 nm(4) in tris-buffer at ambient temperature. Addition of DNA leads to quenching of emission intensity of the complexes. On increasing the concentration of CT DNA, emission intensity of four complexes(1–4) decreases. The quenching of luminescence of complexes by DNA was consistent with a photo electron transfer from the guanine base of DNA to the excited MLCT(Metal ligand charge transfer) state of metal complexes [30–32].

Fluorescence Spectroscopy

The fluorescence quenching experiments were performed to get an estimate on the relative binding affinity of the complexes to CT-DNA with respect to EB. Ethidium bromide (EB) emits intense fluorescence light in the presence of DNA, due to complete intercalation between the adjacent DNA base pairs. It is known that the enhanced fluorescence can be quenched by the addition of a competing agent [33]. The extent of fluorescence of EB bound to DNA, is used to determine the extent of binding between the competing agent and DNA. The emission spectra of EB bound to DNA, in the absence and in the presence of

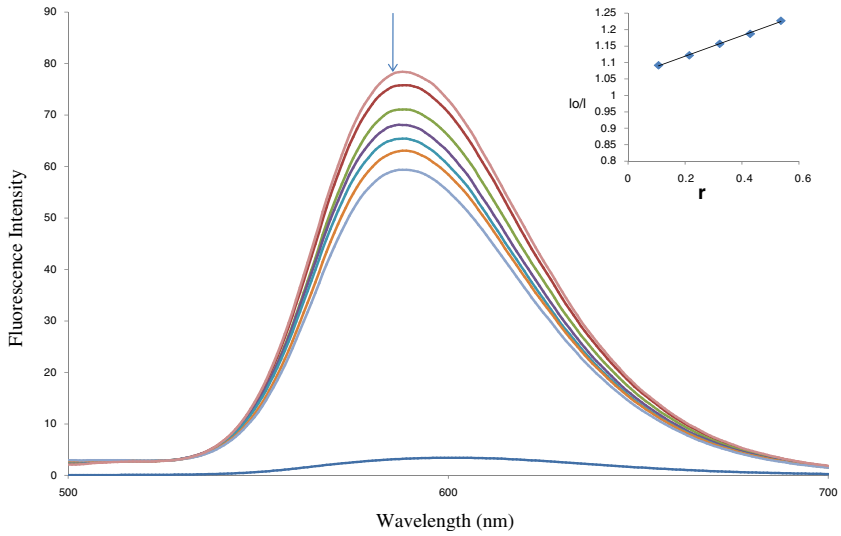

Fig. 9 Emission spectra of EB bound to DNA ([DNA]=2.33×10−5M), in the absence and presence of VO(IV)complex (10 μM) . Inset: Stern-Volmer quenching

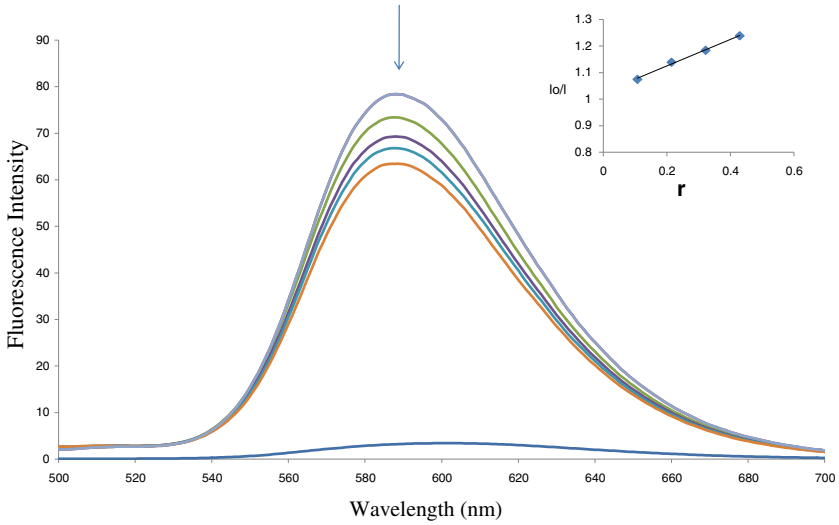

Fig. 10 Emission spectra of EB bound to DNA ([DNA]=2.33×10−5M). in the absence and presence of Fe(III)complex (10 μM) Inset: Stern-Volmer quenching

complexes are given in Figs. 7, 8, 9, and 10. The addition of the complexes to DNA pretreated with EB caused appreciable reduction in emission intensity, indicating that the complexes bind to DNA at the sites occupied by EB. The above data were analysed by means of the Stern-Volmer equation.

The classical Stern—Volmer equation [34] is, $I_o/I=K_r$, where Io and I are the fluorescence intensities in the absence and the presence of complex, respectively, K_r is a linear Stern-Volmer quenching constant dependent on the ratio of r_{EB} (the ratio of the bound concentration of EB to the concentration of DNA) and r is the ratio of total concentration of complex to that of DNA. The fluorescence quenching curves of EB bound to DNA are also shown in Figs. 7, 8, 9, and 10 inset. The quenching plots illustrate, that the quenching of EB bound to DNA by the complexes, are in good agreement with the linear Stern—Volmer equation. It proves that the complexes bind to DNA. In the linear fit plot of I_o/I versus [complex]/[DNA], K is given by the ratio of the slope to the intercept. The K values for complexes with metal ions Co-II, Zn-II, Fe-III and VO-IV, 0.356, 0.210, 0.487, 0.354, respectively. Based on the K values the order of binding strength of metal complexes to CT DNA is found to be Fe-III>Zn-II>VO-IV>Co-II. These results show that all the complexes interact with DNA through minor groove binding. These results should be considered as promising lead compounds for the development of targeted drugs for cancer treatment.

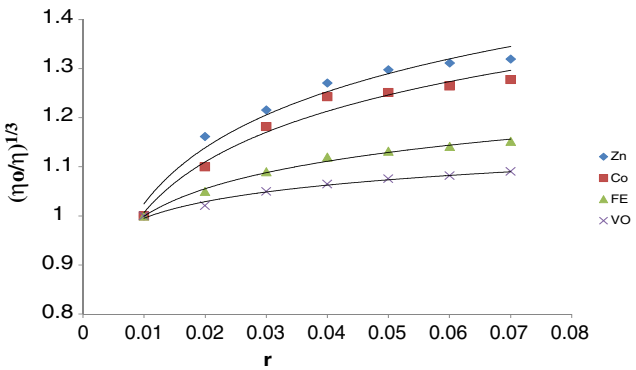

Fig. 11 Effects of increasing amount of EB on complexes Co(II),Zn(II),Fe(III) and VO(IV) on the relative viscosity of CT-DNA at 29 °C±0.1, [DNA]=15 μM

Viscosity Measurements

To authenticate the intercalative binding, viscosity experiments were performed. It is well known that the relative viscosity of CT-DNA solution on interaction with complex will increase for intercalative binding mode, remain same for classical groove binding and decrease for partial intercalation [35–37]. The effect of complexes on the viscosity of DNA depicted in Fig. 11, shows steady increase in the viscosity of the DNA with the addition of increasing amounts of the complexes. Such behaviour is consistent with other intercalaters (i.e., EB), which increase the relative specific viscosity for the lengthening of the DNA double helix resulting from intercalation. The results clearly indicate that all the complexes intercalate between adjacent base pairs, causing an extension in the helix there by increasing the viscosity of DNA.

Conclusions

The metal complexes of Co(II), Ni(II), Zn(II), Fe(III) and VO(IV) and with Schiff base MSALAAAP were synthesized and characterized. The formulations are in accordance with the data of elemental analysis and physicochemical measurements. Based on these observations, the metal ions found to coordinate through phenolic oxygen, azomethine nitrogen of antipyrine ring . These complexes were also found to show significant anti bacterial and DNA binding activity.

Acknowledgments The authors are thankful to Prof. Gopal Reddy, Department of Microbiology, Osmania University, Hyderabad, for his help in antibacterial studies.

References

1. Donia AM, EI-Saled FA (1988) Complexes of manganese(II), cobalt(II) and nickel(II) with the keto form of some antipyrine Schiff base derivatives. Polyhedron 7:2149–2153
2. Joseph M, Nair KM, Radhakrishnan PK (1995) Complexes of yttrium and lanthanide bromides with 4-N-(2′-hydroxybenzylidene) aminoantipyrine. Synth React Inorg Met-Org Chem 25(8):1331–1343
3. Maurya RC, Mishra DD, Trivedi PK, Mukherjee S, Shrivastava PK (1992) Synthesis and characterization of some hovel pehta-coordihated mixed-ligakd derivatives of zinc(II)-bis(acetylacetone) and-bis(acetoacetanilide) chelates with 2/3-pyrazoline-5-one derivatives. Synth React Inorg Met-Org Chem 22(4):403–414
4. Agarwal RK, Singh G (1986) Preparation, spectral and thermal studies of some oxovanadium(IV) complexes of 4-aminoantipyrine. Synth React Inorg Met-Org Chem 16(8):1183–1196
5. Chopra JR, Uppal D, Arrora US, Gupta SK (2000) Synthesis and spectral studies of Cu(II) complexes of 4[N-(2-hydroxy-1-naphthalidene) amino]antipyrine thiosemicarbazones. Asian J Chem 12:1277–1281
6. Radhakrishnan PK, Indrasenan P, Nair CGR (1984) Complexes of lanthanide nitrates with 4n-(2′-hydroxy benzylidene)-aminoantipyrine. Polyhedron 3:67–70
7. Radhakrishnan PK (1986) complexes of lanthanide perchlorates with 4-*N*-(2′-hydroxy-1′-naphthylidene)aminoantipyrine. Polyhedron 5: 995–998
8. Maurya RC, Mishra DD, Pandey M, Shukla P, Rathour R (1993) Synthesis and spectral studies of octacoordinated dioxouranium(VI) complexes with some schiff bases derived from 4-acetyl-2,3-dimethyl-l-(4-methylphenyl)-3-pyrazoline-5-one and aromatic amines. Synth React Inorg Met-Org Chem 23(1):161–174
9. Ismail KZ, EI-Dissouky A, Shehada AZ (1997) Spectroscopic and magnetic studies on some copper(II) complexes of antipyrine Schiff base derivatives. Polyhedron 16:2909–2916
10. Agarwal RK, Garg P, Agarwal H, Chandra J (1997) Synthesis, magneto-spectral and thermal studies of cobalt(II) and nickel(II) complexes of 4-[N-(4-dimethylaminobenzylidene) amino] antipyrine. Synth React Inorg Met-Org Chem 27(2):251–268
11. Singh L, Tyagi N, Dhaka NP, Sindhu SK (1999) Synthesis, spectral and thermal studies of some lanthanide(III) complexes of 4-[-N-(benzalidene) amino]antipyrine thiosemicarbazones. Asian J Chem 11:503–508
12. Agarwal RK, Prakash J (1991) Synthesis and characterization of thorium(IV) and dioxouranium(VI) complexes of 4-[N(2-hydroxy-1-naphthalidene)amino]antipyrine. Polyhedron 10:2399–2403
13. Shankar G, Prem kumar RR, Ramalingam SK (1986) 4-Aminoantipyrine Schiff-base complexes of lanthanide and uranyl ions. Polyhedron 5:991–994
14. Kuncheria B, Indrasenan P (1988) Thorium(IV) nitrate complexes with some Schiff bases of 4-aminoantipyrine and certain carbonyl compounds. Polyhedron 7:143–146
15. Thomas M, Nair KM, Radhakrishanan PK (1995) Rare earth iodide complexes of 4-(2′,4′-dihydroxyphenylazo) antipyrine. Synth React Inorg Met-Org Chem 25(3):471–479
16. Surendra Babu MS, Hussain Reddy K, Krishna PG (2007) Synthesis, characterization, DNA interaction and cleavage activity of new mixed ligand copper(II) complexes with heterocyclic bases. Polyhedron 26(3):572
17. Anupama B, Mounika K, Sunitha M, Venkata Ramana Reddy C, Gyana Kumari C (2012) Synthesis, characterization and biological activity of metal complexes with 4-aminoantipyrine Schiff bases of 5-chloro salicylaldehyde and 3-ethoxy salicylaldehyde. J Indian Chem Soc 89:735–743
18. Geary WG (1971) Coord Rev 7:81
19. Sece JM, Quiros M, Garmendina MJG (2000) Synthesis, X-ray crystal structure and spectroscopic, magnetic and EPR studies of copper(II) dimers with methoxy-di-(2-pyridyl)methoxide as bridging ligand. Polyhedron 19:1005–1013
20. Alemi AA, Shaabani B (2000) Synthesis and characterization of a Schiff base of P-tert butylcalix[4]arene and its complex with copper(II). Acta Chim Slov 47:363–369
21. Chang CJ, Connick WB, Low DW, Day MW, Gray HB (1998) Electronic structures of nitridomanganese(V) complexes. Inorg Chem 37:3107–3110
22. Mashalay MM (1996) Synthesis and physico-chemical studies on rhenium(V) complexes with 2-benzimidazolethione. Synth React Inorg Met-Org Chem 26:211–224
23. Mashalay MM (2002) Preparation and thermal studies of some new oxorhenium(V) complexes with 2-amino-5-methyl-1,3,4-thiadiazole. Synth React Inorg Met-Org Chem 32:373–397
24. Raman N, Kulandaisamy A, Jeyasubramanian K (2001) Synthesis, spectroscopic characterization, redox and biological screening studies of some Schiff base transition metal(II) complexes derived from salicylidene-4-aminoantipyrine and 2-aminophenol/2-aminothiophenol. Synth React Inorg Met Org Chem 31(7):1249–1270
25. Nakamoto K (1997) Infrared and raman spectra of inorganic and coordination compounds, 3rd edn. Wiley, New York
26. Maurya RC, Sharma P (1999) Synthesis, magnetic and spectral studies of Co(II) pictrate complexes with heterocyclic nitrogen donors. Ind J Chem 38A:509–513
27. Raman N, Kulaindaisamy A, Jeyasubramanian K (2002) Synthesis, spectral, redox and antimicrobial activity of Schiff base transition metal(II) complexes derived from 4-aminoantipyrine and benzil. Synth React Inorg Met Org and Nano-Metal Chem 32(9):1583–1610
28. Nikolaev AV, Myachina LI, Logvinenko VA (1969) Therm Anal 2: 779
29. Dharmaraj N, Vishwanathanmurthi P, Natarajan K (2001) Ruthenium(II) complexes containing bidentate Schiff bases and their antifungal activity. Transit Met Chem 26:105–109
30. Vaidyanathan VG, Nair BU (2003) Photooxidation of DNA by cobalt(II) tridentate complex. J Inorg Biochem 94:121–126
31. Kelly JM, Mc Cintoonnell DJ, Oh Uigin C, Tossi AB, Kirsch-De Mesmaeker A, Masschelein A, Nasielski J (1987) Ruthenium polypyridyl complexes; their interaction with DNA and their role as senstisers for its photocleavage. J Chem Soc Chem Commun 24: 1821–1823
32. Vaidyanathan VG, Nair BU (2005) Synthesis, characterization and electrochemical studies of mixed ligand complexes ruthenium (II) with DNA. Dalton Trans:2842–2848
33. Wolf A, Shimer GH Jr, Meehan T (1987) Polycyclic aromatic hydrocarbons physically intercalate duplex regions of denatured DNA. Biochemistry 12:4161–4170
34. Baguley BC, Le Bret M (1984) Quenching of DNA-ethidium flurescence by amacrine and other antitumour agents: a possible electron–transfer effect. Biochemistry 23:937–943
35. Lakowicz JR, Weber G (1973) Quenching of fluorescence by oxygen, a probe for structural fluctuations in macromolecules. Biochemistry 12:4161–4170
36. Sathyanarayana S, Dabrowiak JC, Chairs JB (1992) Neither DELTA -nor LAMBDA -Tris (phenantroline) ruthenium(II) binds to DNA by classical intercalation. Biochemistry 31:9319–9322
37. Sunita M, Padmaja M, Anupama B, Gyanakumari C (2012) Synthesis, characterization, DNA binding and cleavage studies of mixed ligand Cu(II) complexes of 2,6-bis(benzimidazol-2-yl)pyridine. J Fluoresc 22:1003–1012